J|A|C|S
ARTICLES
Published on Web 09/09/2003

The Rate of O_2 and CO Binding to a Copper Complex, Determined by a "Flash-and-Trap" Technique, Exceeds that for Hemes

H. Christopher Fry, Donald V. Scaltrito, Kenneth D. Karlin,* and Gerald J. Meyer*

Contribution from the Johns Hopkins University, Department of Chemistry, 3400 N. Charles Street, Baltimore, Maryland 21218

Received February 27, 2003; E-mail: karlin@jhu.edu, meyer@jhu.edu

Abstract: The observation and fast time-scale kinetic determination of a primary dioxygen−copper interaction have been studied. The ability to photorelease carbon monoxide from $[Cu^{I}(tmpa)(CO)]^{+}$ in mixtures of CO and O_2 in tetrahydrofuran (THF) between 188 and 218 K results in the observable formation of a copper-superoxide species, $[Cu^{II}(tmpa)(O_2^{-})]^{+}$ $\lambda_{max} = 425$ nm. Via this "flash-and-trap" technique, temperature-dependent kinetic studies on the forward reaction between dioxygen and $[Cu^{I}(tmpa)(thf)]^{+}$ afford activation parameters $\Delta H^{\ddagger} = 7.62$ kJ/mol and $\Delta S^{\ddagger} = -45.1$ J/mol K. The corresponding reverse reaction proceeds with $\Delta H^{\ddagger} = 58.0$ kJ/mol and $\Delta S^{\ddagger} = 105$ J/mol K. Overall thermodynamic parameters are $\Delta H^{\circ} = -48.5$ kJ/mol and $\Delta S^{\circ} = -140$ J/mol K. The temperature-dependent data allowed us to determine the room-temperature second-order rate constant, $k_{O2} = 1.3 \times 10^{9}$ M^{-1} s^{-1}. Comparisons to copper and heme proteins and synthetic complexes are discussed.

Introduction

Copper-mediated oxidative chemistry is important for practical applications and in bioinorganic processes.[1−5] For the latter, Cu(I)/dioxygen interactions are known or implicated for a variety of copper proteins, such as hemocyanins (O_2-carriers), monooxygenases, and heme-copper oxidases.[2−6] Thus, fundamental information on the primary interaction of O_2 with copper(I) in proteins and complexes is of considerable importance. In addition, comparison of such chemistry to hemes (iron-porphyrinates) in proteins or model compounds is also of interest.[7−9]

$[Cu^{I}(tmpa)(CH_3CN)]^{+}$ (tmpa = tris(2-pyridylmethyl)amine; $\lambda_{max} = 338$ nm, $\epsilon = 5600$ M^{-1} cm^{-1}) has been shown to react rapidly with dioxygen in propionitrile (EtCN) solvent forming the 1:1 adduct $[Cu^{II}(tmpa)(O_2^{-})]^{+}$, a cupric-superoxo species ($\lambda_{max} = 410$ nm, $\epsilon = 4700$ M^{-1} cm^{-1}).[7,10] $[Cu^{II}(tmpa)(O_2^{-})]^{+}$ further reacts with a second equivalent of $[Cu^{I}(tmpa)(RCN)]^{+}$ to form the μ-1,2 peroxo species $[\{Cu^{II}(tmpa)\}_2(O_2^{2-})]^{2+}$ ($\lambda_{max} = 525$ nm, Scheme 1). Stopped-flow kinetic measurements showed that for the primary $[Cu^{I}(tmpa)(RCN)]^{+}/O_2$ reaction, $k_{O2} = 5.8 \times 10^{7}$ M^{-1} s^{-1}, $k_{-O2} = 1.5 \times 10^{8}$ s^{-1} (extrapolated to 298 K from variable, low-temperature data).[7,11] The EtCN solvent competes strongly with O_2 for interaction/binding with copper(I), however in weakly coordinating, noncompeting solvents such as tetrahydrofuran (THF), the superoxide species $[Cu^{II}(tmpa)(O_2^{-})]^{+}$ forms within the mixing time of the stopped-flow instrument, even at 183 K, $k_{O2} > 10^{6}$ M^{-1} s^{-1}.[11]

Scheme 1

$$LM + O_2 \rightleftharpoons LM^{+}(O_2^{-})$$

$$LM + LM^{+}(O_2^{-}) \rightleftharpoons \{LM^{+}\}_2(O_2^{2-})$$

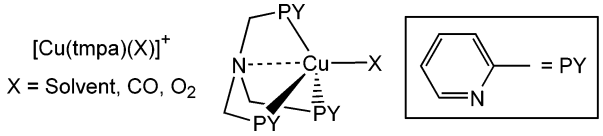

On a similar note, cobalt complexes have long been studied to understand fundamental transition metal dioxygen interactions.[9] Earlier work with cobalt(II) using the macrocyclic ligand [14]aneN$_4$,[12] displays cobalt-dioxygen chemistry identical to our $[Cu^{I}(tmpa)(Solvent)]^{+}$ system described above (Scheme 1). Stopped-flow and photochemical methods were used to study the Co/O_2 reaction.[12,13] The ability to photohomolytically cleave the Co−O_2 bond in $[([14]aneN_4)Co^{III}(O_2^{-})]^{2+}$ and observe the subsequent recombination of dioxygen with the reduced cobalt species yielded an accurately measured second-order rate constant, $k_{O2} = 1.2 \times 10^{7}$ M^{-1} s^{-1}.[13]

To this point, primary copper-dioxygen interactions have not been determined on sub-microsecond time scales. Yet, such

(1) Que, L., Jr.; Tolman, W. B. *Angew. Chem., Int. Ed. Engl.* **2002**, *41*, 1114−1137.
(2) Zhang, C. X.; Liang, H.-C.; Humphreys, K. J.; Karlin, K. D. In *Catalytic Activation of Dioxygen by Metal Complexes*; Simandi, L., Ed.; Kluwer: Dordrecht, The Netherlands, 2003; pp Chapter 2, pp 79−121.
(3) Solomon, E. I.; Chen, P.; Metz, M.; Lee, S.-K.; Palmer, A. E. *Angew. Chem., Int. Ed. Engl.* **2001**, *40*, 4570−4590.
(4) Solomon, E. I.; Sundaram, U. M.; Machonkin, T. E. *Chem. Rev.* **1996**, *96*, 2563−2605.
(5) Klinman, J. P. *Chem. Rev.* **1996**, *96*, 2541−2561.
(6) Ferguson-Miller, S.; Babcock, G. T. *Chem. Rev.* **1996**, *96*, 2889−2907.
(7) Karlin, K. D.; Kaderli, S.; Zuberbühler, A. D. *Acc. Chem. Res.* **1997**, *30*, 139−147.
(8) Momenteau, M.; Reed, C. A. *Chem. Rev.* **1994**, *94*, 659−698.
(9) Bakac, A. *Prog. Inorg. Chem.* **1995**, *43*, 267−351.
(10) Tyeklár, Z.; Jacobson, R. R.; Wei, N.; Murthy, N. N.; Zubieta, J.; Karlin, K. D. *J. Am. Chem. Soc.* **1993**, *115*, 2677−2689.
(11) Zhang, C. X.; Kaderli, S.; Costas, M.; Kim, E.-i.; Neuhold, Y.-M.; Karlin, K. D.; Zuberbühler, A. D. *Inorg. Chem.* **2003**, 1807−1824.
(12) Wong, C.-L.; Switzer, J. A.; Balakrishnan, K. P.; Endicott, J. F. *J. Am. Chem. Soc.* **1980**, *102*, 5511−5518.
(13) Bakac, A.; Espenson, J. H. *J. Am. Chem. Soc.* **1990**, *112*, 2273−2278.

10.1021/ja034911v CCC: $25.00

information has long been available for hemes, using techniques originally developed by Gibson and co-workers,[14,15] as well as diffusion controlled "flash-and-trap" experiments.[8] The photoinitated ejection of carbon monoxide from heme-CO adducts in the presence of dioxygen has led to a wealth of important information for proteins such as hemoglobin, myoglobin, and cytochrome *c* oxidase,[6,16−23] as well as synthetic iron-porphyrinate model compounds.[8,24,25]

Previously, we reported the ability to photolytically remove a single carbon monoxide molecule from $[Cu^I(tmpa)(CO)]^+$ in various solvents via metal-to-ligand charge transfer (MLCT) excitation.[26] In these experiments, we monitored the fast recombination of CO and the copper complex. Here, for the first time, we use this ability to perform a novel copper "flash-and-trap" experiment, typically used for hemes, leading to the accurate determination of the second-order rate constant for (ligand)Cu/O_2 reaction, found to be in excess of 10^9 M^{-1} s^{-1} at 298 K. This value exceeds that for synthetic and natural hemes.

Experimental Section

Synthesis of $[Cu^I(tmpa)(CO)]B(C_6F_5)_4$. $[Cu^I(CH_3CN)_4]B(C_6F_5)_4$[27] and TMPA[28] were prepared according to literature procedures. In a 100 mL Schlenck flask equipped with a stir bar $[Cu^I(CH_3CN)_4]B(C_6F_5)_4$ (198 mg, 213 mmol) and TMPA (63 mg, 217 mmol) were added. CO was bubbled through dry diethyl ether (5 mL) for 15 min and added dropwise to the mixture under an atmosphere of CO. The solution was stirred for 1 h while dry heptane (100 mL) was bubbled with CO. The heptane was added to the stirring solution affording a white precipitate. The supernatant was removed via cannula and the product was dried in vacuo yielding an off-white powder (75%). Elemental Analysis: Calculated: C, 48.68; H, 1.71; N, 5.28, Experimental: C, 48.50; H, 1.89; N, 4.49. IR Nujol mull ν_{CO} = 2077 cm^{-1}.

Mixing Carbon Monoxide and Dioxygen. An MKS Instruments Multi Gas Controller (MGC, MKS 647C) was used to control the flow of carbon monoxide and dioxygen through two MKS Instruments mass flow controllers (MFCs, MKS 1179A). The MFCs have a maximum flow rate of 200 standard cubic centimeter per minute (sccm). Gas correction factors (GCFs) programmed into the MGC were utilized to correct for specific heat, density, and the molecular structure of the gases. The two gases here have a gas correction factor of 1.00 (nitrogen is the standard having a GCF of 1.00) meaning if the flow rate of CO and O_2 are equal then the ratio of gas being added is 1:1. Carbon monoxide and dioxygen were varied in such a manner that the gas mixture's total flow rate was 100 sccm (i.e. If the CO flow rate was set to 30 sccm, then the O_2 flow rate was set to 70 sccm for a 3:7 CO:O_2 mixture).

Determination of Carbon Monoxide and Dioxygen Concentrations. First, the solubility of gases in THF were determined using mole fractions and temperature-dependent data given in the literature.[29,30] CO at atmospheric pressure in THF has a solubility of 0.0109 M in THF at RT. O_2 at atmospheric pressure in THF has a solubility of 0.0101 M in THF at RT. (Newer dioxygen solubility (THF, 25 °C) values are available: 0.0066 M[11] and 0.0087 M (LTP GmbH, University of Oldenburg, Germany; to be published). However, here we use the older literature value.[30]) By varying the ratio of CO and O_2 with the MGC, the concentration of the gases were determined simply by taking the percentage of the gas added and multiplying by the solubility of the corresponding gas in THF (For example, if the CO:O_2 flow rate is 3:7 (or 30% of the total gas flow is CO), then the concentration of CO in THF = 0.30 × 0.0109 M = 0.0033 M and O_2 = 0.70 × 0.0101 M = 0.0070 M).

Low Temperature, Gas Mixing, Flash Photolysis Methods. Experimental information for the setup of the Nd:YAG flash photolysis apparatus has been previously reported.[31] The following modifications were made. A Neslab ULT-95 Low-Temperature Circulating Methanol Bath was used to control the temperature through a four-window UV−vis Dewar (M. S. Marten) filled with methanol specifically designed for these experiments. Due to the use of CO, a Plexiglas "portable" exhaust hood with an aluminum frame and exhaust fan fixed at the top was constructed (Figure S1) to fit around the Dewar. Appropriate apertures were cut into the Plexiglas for plumbing from the low-temperature apparatus, tubing from the gas mixer, and for the pump and probe beams.

Sample Preparation, Incorporation of Gas Mixtures, and Flash Photolysis Conditions. To a Schlenck quartz cuvette (10 mm, with four clear sides) designed for low-temperature studies was added a 0.2−0.6 mM solution of $[Cu^I(tmpa)(CO)]B(C_6F_5)_4$ in dried and degassed THF. Note: It is known that when $[Cu^I(tmpa)(CO)]B(C_6F_5)_4$ is added to either THF or nitrile solvents the CO ligand dissociates. The Schlenck cuvette equipped with a 14/20 rubber stopper was then placed under 1 atm of CO via direct bubbling into the solution with a needle and placed in the low-temperature dewar and aligned with the pump and probe beams. CO:O_2 gas mixtures (ranging from 60:40 to 10:90 ratios varied in increments of 5) were added via direct bubbling through the solution with a needle for 10 min. Once the solution was purged, the gas was allowed to flow openly in the headspace to ensure maintenance of the mixture and atmospheric pressure. The sample was irradiated with 355 nm light at 10 mJ/pulse.

(14) Gibson, Q. H.; Greenwood, C. *Biochem. J.* **1963**, *86*, 541−554.
(15) Greenwood, Ç.; Gibson, Q. H. *J. Biol. Chem.* **1967**, *242*, 1782−1787.
(16) Einarsdóttir, O.; Dyer, R. L.; Lemon, D. D.; Killough, P. M.; Hubig, S. M.; Atherton, S. J.; López-Garriga, J. J.; Palmer, G.; Woodruff, W. H. *Biochemistry* **1993**, *32*, 12 013−12 024.
(17) Han, S.; Takahashi, S.; Rousseau, D. L. *J. Biol. Chem.* **2000**, *275*, 1910−1919.
(18) Szundi, I.; Liao, G.-L.; Einarsdottir, O. *Biochemistry* **2001**, *40*, 2332−2339.
(19) Stavrakis, S.; Koutsoupakis, K.; Pinakoulaki, E.; Urbani, A.; Saraste, M.; Varotsis, C. *J. Am. Chem. Soc.* **2002**, *124*, 3814−3815.
(20) Heitbrink, D.; Sigurdson, H.; Bolwien, C.; Brzezinski, P.; Heberle, J. *Biophysical Journal* **2002**, *82*, 1−10.
(21) Okuno, D.; Iwase, T.; Shinzawa-Itoh, K.; Yoshikawa, S.; Kitagawa, T. *J. Am. Chem. Soc.* **2003**, *125*, 7209−7218.
(22) Bailey, J. A.; Tomson, F. L.; Mecklenburg, S. L.; MacDonald, G. M.; Katsonouri, A.; Puustinen, A.; Gennis, R.; Woodruff, W. H.; Dyer, R. B. *Biochemistry* **2002**, *41*, 2675−2683.
(23) Liebl, U.; Lipowski, G.; Négrerie, M.; Lambry, J.-C.; Martin, J.-L.; Vos, M. H. *Nature* **1999**, *401*, 181−184.
(24) David, S.; James, B. R.; Dolphin, D.; Traylor, T. G.; Lopez, M. A. *J. Am. Chem. Soc.* **1994**, *116*, 6−14.
(25) Collman, J. P.; Brauman, J. I.; Iverson, B. L.; Sessler, J.; Morris, R. M.; Gibson, Q. H. *J. Am. Chem. Soc.* **1983**, *105*, 3052−3064.
(26) Scaltrito, D. V.; Fry, H. C.; Showalter, B. M.; Thompson, D. W.; Liang, H.-C.; Zhang, C. X.; Kretzer, R. M.; Kim, E.-i.; Toscano, J. P.; Karlin, K. D.; Meyer, G. J. *Inorg. Chem.* **2001**, *40*, 4514−4515.
(27) Liang, H.-C.; Kim, E.; Incarvito, C. D.; Rheingold, A. L.; Karlin, K. D. *Inorg. Chem.* **2002**, *41*, 2209−2212.
(28) Jacobson, R. R. Ph.D. Thesis, State University of New York at Albany, 1989.
(29) Payne, M. W.; Leussing, D. L.; Shore, S. G. *J. Am. Chem. Soc.* **1987**, *109*, 617−618.
(30) Battino, R. *IUPAC Solubility Data Series: Oxygen and Ozone*; Pergamon: Oxford, New York, 1981.
(31) Argazzi, R.; Bignozzi, C. A.; Heimer, T. A.; Castellano, F. N.; Meyer, G. J. *J. Phys. Chem.* **1994**, *33*, 5741−5749.

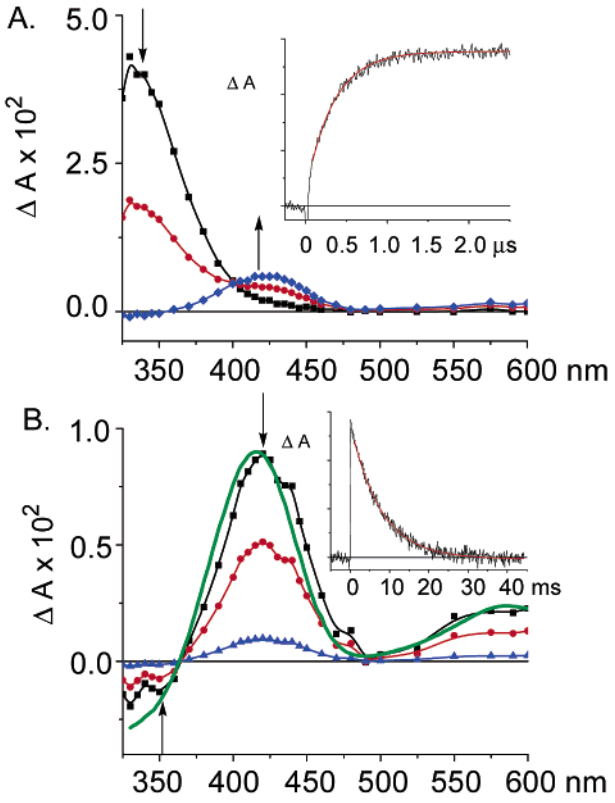

Figure 1. Difference spectra $\{[Cu(tmpa)(X)]^+ - [Cu^I(tmpa)(CO)]^+\}$ recorded after pulsed 355 nm excitation of $[Cu^I(tmpa)(CO)]^+$ in THF at 198 K under a 1 atm O_2:CO (7:3) mixture. The spectra were recorded at various delay times: (A) 0 to 2 μs representing the conversion of $[Cu^I(tmpa)(thf)]^+$ (λ_{max}, 333 nm) to a mixture of $[Cu^I(tmpa)(CO)]^+$ and $[Cu^{II}(tmpa)(O_2^-)]^+$ (λ_{max} = 425 nm): squares (black spectrum), 0 μs; circles (red spectrum), 0.5 μs; diamonds (blue spectrum), 2.0 μs. The inset is an absorption transient monitored at 425 nm with a superimposed first-order fit (in red), $k_{obs} = 3.0 \times 10^6$ s^{-1} and (B) 2 μs to 40 ms representing the conversion from $[Cu^{II}(tmpa)(O_2^-)]^+$ to $[Cu^I(tmpa)(CO)]^+$: squares (black spectrum), 2 μs; circles (red spectrum) 5 ms; diamonds (blue spectrum), 20 ms. The inset is an absorption transient monitored at 425 nm with a superimposed first-order fit, $k_{obs} = 130$ s^{-1}. For comparison, the spectrum calculated as $\{Abs[Cu^{II}(tmpa)(O_2^-)]^+ - Abs[Cu^I(tmpa)(CO)]^+\}$ is shown in solid green.

An average of 60 transient kinetic traces was taken per wavelength observed (330 to 600 nm in 5 nm increments).

Results

We recently demonstrated the ability of the copper−carbonyl complex $[Cu^I(tmpa)(CO)]^+$ ($\lambda_{shoulder}$ = 350 nm, ϵ = 1200 M^{-1} cm^{-1}) to photorelease carbon monoxide.[26] As is observed for many heme proteins or complexes where CO binding to the reduced metal ion (Fe(II)) protects against rapid O_2-reaction,[8,24,25] $[Cu^I(tmpa)(CO)]^+$ in THF solvent is inert when mixtures of dioxygen and carbon monoxide are introduced at low temperatures (188−218 K). Under these conditions, light excitation (λ_{ex} = 355 nm, 8−10 ns pulse)[31] into the $[Cu^I(tmpa)(CO)]^+$ metal-to-ligand charge transfer (MLCT) band results in the immediate (within 10 ns) formation of the solvated species $[Cu^I(tmpa)(thf)]^+$ (λ_{max} = 333 nm; Figure 1A) as previously observed.[26] Subsequently, fast competing reactions occur (k_{fast}, s^{-1}, Scheme 2), either regenerating $[Cu^I(tmpa)(CO)]^+$ [26] or forming $[Cu^{II}(tmpa)(O_2^-)]^+$ (λ_{max} = 425 nm, 600 nm in THF).[11] Supporting observations are as follows: (i) the generation of $[Cu^{II}(tmpa)(O_2^-)]^+$ is O_2-dependent and its rate of formation

Scheme 2

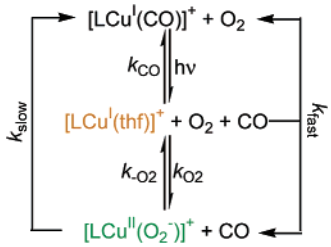

exactly parallels the rate of disappearance of $[Cu^I(tmpa)(thf)]^+$ ($k_{fast} = 3 \times 10^6$ s^{-1}, for $[O_2]/[CO]$ = 7:3), Figure 1A, (ii) $[Cu^{II}(tmpa)(O_2^-)]^+$ forms in ~20% yield ($[O_2]/[CO]$ = 7:3)[32] consistent with competition of $[Cu^I(tmpa)(thf)]^+$ for reaction with either CO or O_2, (iii) the k_{fast} value linearly decreases as $[O_2]$ is increased, confirming the O_2-dependence and the presence of competitive reactions (Figure 2) and thus the k_{fast} is a combination of two rate constants (eq 1), and CO rebinding dominates over O_2-binding to $[Cu^I(tmpa)(thf)]^+$, $k_{CO} > k_{O2}$ (Scheme 2)

$$k_{fast} = k_{CO}[CO] + k_{O2}[O_2] \quad (1)$$

Values for k_{CO} were determined in the absence of dioxygen. The rate constant for the O_2-reaction was thus determined from the slope of the plot, $k_{fast} - k_{CO}[CO]$ vs $[O_2]$ (Figure 2).

Further analysis reveals a second, slower reaction (Figure 1B), the equilibration from $[Cu^{II}(tmpa)(O_2^-)]^+$ back to $[Cu^I(tmpa)(CO)]^+$ (k_{slow}, Scheme 2) completing a fully reversible process. A plot of $1/k_{slow}$ vs $[O_2]/[CO]$ (Figure 2), often employed to analyze the analogous dissociative reaction in heme systems,[8,33] readily leads to K_{O2} (= k_{O2}/k_{-O2}) and k_{-O2} (eq 2). From this 'slow' analysis, k_{O2} was calculated (Table 1) and determined to be in close agreement with the rate constant obtained from the fast reaction analysis (vide supra).

$$\frac{1}{k_{slow}} = \frac{K_{O2}[O_2]}{k_{CO}[CO]} + \frac{1}{k_{-O2}} \quad (2)$$

Temperature-dependent studies afforded both activation (Eyring analysis) and thermodynamic (Van't Hoff analysis) parameters for the dioxygen binding process.[34] Analysis of both the "fast" and "slow" processes provided data for the forward reaction (k_{O2}) which displayed a temperature dependence, $\Delta H^{\ddagger} = 7.62$ kJ mol^{-1} and $\Delta S^{\ddagger} = -45.1$ J mol^{-1} K^{-1}. Data corresponding to the reverse reaction (k_{-O2}) were obtained from the "slow" process (Scheme 2) and displayed a greater temperature dependence, $\Delta H^{\ddagger} = 58.0$ kJ mol^{-1} and $\Delta S^{\ddagger} = 105$ J mol^{-1} K^{-1}. The thermodynamic parameters were also obtained from the "slow" process, $\Delta H^{\circ} = -48.5$ kJ mol^{-1} and $\Delta S^{\circ} = -140$ J mol^{-1} K^{-1}. Thus, we could extrapolate to room temperature (298 K) to give data averaged values (Table 1): $k_{O2} = 1.3 \times 10^9$ M^{-1} s^{-1}, $k_{-O2} = 1.5 \times 10^8$ M^{-1} s^{-1}, and $K_{O2} = 15.4$ M^{-1}.[35]

Discussion

1:1 Copper Dioxygen Interactions: Kinetic and Thermodynamic Parameters. We have directly determined the fastest

(32) The yield was obtained by utilizing the extinction coefficient for $[Cu(tmpa)(O_2^-)]^+$ in THF from stopped-flow measurements (refs 7, 11).
(33) Antonini, E.; Brunori, M. *Hemoglobin and Myoglobin in Their Reactions with Ligands*; North-Holland Publishing Co.: Amsterdam, 1971.
(34) See the Supporting Information online.
(35) The k_{O2} would in fact be greater (i.e., 1.9×10^9 M^{-1} s^{-1}) if we employed the more recently reported value for O_2 solubility in THF;[11] also see Experimental section for further notes.

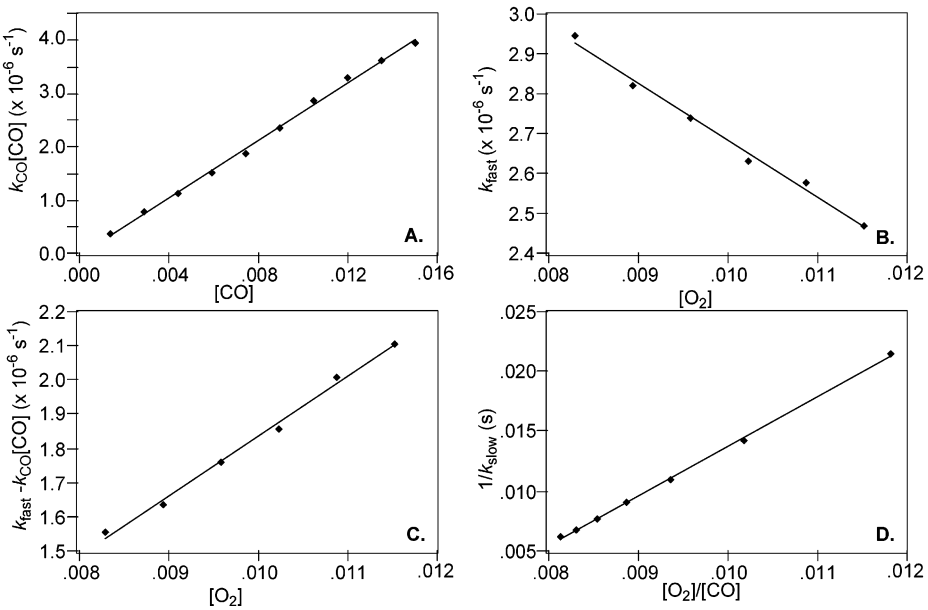

Figure 2. Gas concentration dependence of the fast (A−C) and slow (D) processes in THF at 198 K. (A) CO dependence in the absence of dioxygen (k_{CO}[CO] versus [CO]) pertaining to the recombination of CO to $[Cu^{I}(tmpa)(thf)]^{+}$. (B) O_2 dependence (k_{fast} versus $[O_2]$) pertaining to the competitive recombination of CO and O_2 to $[Cu^{I}(tmpa)(thf)]^{+}$. (C) O_2 dependence of the corrected rate constant ($k_{O2}[O_2] = k_{fast} - k_{CO}[CO]$ versus $[O_2]$). (D) Plot of $1/k_{slow}$ versus $[O_2]/[CO]$ corresponding to the slow equilibration from $[Cu^{II}(tmpa)(O_2^{-})]^{+}$ to $[Cu^{I}(tmpa)(CO)]^{+}$.

Table 1. Comparison of Thermodynamic and Kinetic Parameters for the Binding of O_2 to Copper Complexes

parameter	$[Cu^{I}(tmpa)(thf)]^{+}$	$[Cu^{I}(tmpa)(EtCN)]^{+}$ [11]	$[Cu^{I}(Me_6tren)(EtCN)]^{+}$ [38]
k_{O2}, 193 K (M^{-1} s^{-1})	1.6×10^{8} [a]		
	1.4×10^{8} [b]	3.8×10^{4}	1.8×10^{5}
	1.5×10^{8} [c]		
k_{O2}, 298 K (M^{-1} s^{-1})	1.3×10^{9} [c]	5.8×10^{7}	1.2×10^{7}
$\Delta H^{\ddagger}$ (kJ mol^{-1})	7.62	31.6	17.1
$\Delta S^{\ddagger}$ (J mol^{-1} K^{-1})	−45.1	10	−52
k_{-O2}, 193 K (s^{-1})	240 [b]	130	0.62
k_{-O2}, 298 K (s^{-1})	1.3×10^{8} [b]	1.5×10^{8}	7.7×10^{5}
$\Delta H^{\ddagger}$ (kJ mol^{-1})	58.0	61.5	62.0
$\Delta S^{\ddagger}$ (J mol^{-1} K^{-1})	105	118	76
K_{O2}, 193 K (M^{-1})	6.5×10^{5} [b]	260	2.9×10^{5}
K_{O2}, 298 K (M^{-1})	15.4 [b]	0.38	15.5
$\Delta H°$ (kJ mol^{-1})	−48.5	−29.8	−44.9
$\Delta S°$ (J mol^{-1} K^{-1})	−140	−108	−128

[a] Averaged values from the "fast" analysis (two trials). [b] Averaged values from the "slow" analysis (two trials). [c] Averaged values from the "fast" and "slow" analysis (two trials for each).

rate constant for a copper dioxygen interaction using a method previously restricted to hemes. An interesting point is the dynamics of this reaction in various solvents. Although inspiration for the present study stemmed from heme-CO flash experiments, we were in part motivated by our inability to observe the kinetics of $[Cu^{I}(tmpa)(Solvent)]^{+}/O_2$ in noncoordinating solvents on a stopped-flow time scale.[11] The O_2 binding in EtCN solvent has $k_{O2} = 5.8 \times 10^{7}$ M^{-1} s^{-1} (extrapolated to 298 K), which is twenty-two times smaller than the value we report here for THF solvent (Table 1). Temperature dependences indicate an enthalpy of activation four times greater in EtCN than in THF. Thus, at low temperature, EtCN significantly stunts the reaction where $k_{O2} = 3.8 \times 10^{4}$ M^{-1} s^{-1} (193 K) compared to 1.5×10^{8} M^{-1} s^{-1} (THF, 193 K). Such behavior is expected because nitriles are strong Cu(I) ligands and act as severe inhibitors for the binding of dioxygen.[36,37] The entropy of activation in EtCN is 10 J mol^{-1} K^{-1} which has been attributed to a dissociative mechanism, requiring deligation of RCN prior

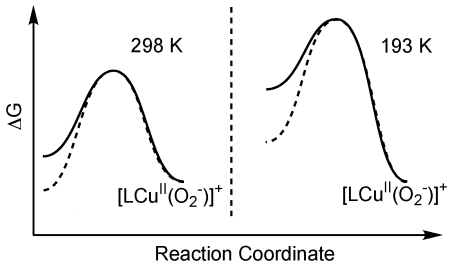

Figure 3. Reaction coordinate diagrams pertaining to dioxygen binding to $[Cu^{I}(tmpa)(Solvent)]^{+}$ at 298 and 193 K (− THF and - - -EtCN).

to O_2-binding.[11] However, in THF, the entropy of activation is negative, −45.1 J mol^{-1} K^{-1} suggesting an associative mechanism or a transition state that is closer in appearance to the final superoxide species. Consequently, in THF, without the interference of a coordinating solvent, the very low activation enthalpy ($\Delta H^{\ddagger} = 7.62$ kJ/mol K) and negative $\Delta S^{\ddagger}$ indicate O_2-binding is basically unhindered.

The dissociation rate constants of dioxygen (k_{-O2}) vary only slightly when changing solvents, consistent with the kinetic/thermodynamic parameters obtained and thus, the dissociation of O_2 depends solely on the $Cu-O_2$ bond breaking process. From the binding constants at room temperature, we see that in THF the O_2-adduct is favored ($K_{O2} = 15.4$ M^{-1}), whereas in EtCN, the solvated, unreacted Cu(I) complex is preferred ($K_{O2} = 0.38$ M^{-1}). At low temperatures, the superoxide is the dominant species in both THF and EtCN ($K_{O2} = 6.5 \times 10^{5}$ M^{-1}, and 260 M^{-1}, respectively) but is more stable in THF.

A simplified reaction coordinate diagram is shown in Figure 3 summarizing the kinetic and thermodynamic situation, showing that the solvent used dictates the rate of the forward reaction (k_{O2}). EtCN clearly has the greater affect on the system as it can coordinate to the reduced species, hindering the forward

(36) Hathaway, B. J. In *Comprehensive Coordination Chemistry*; Wilkinson, G., Ed.; Pergamon: New York, 1987; Vol. 5, pp 533−774.
(37) Jardine, F. H. *Adv. Inorg. Chem. Radiochem.* **1975**, *17*, 115−163.

Table 2. Kinetic and Thermodynamic Parameters for Cu^I/O_2 Reactions (298 K)

compd	k_{O2} (M^{-1} s^{-1})	k_{-O2} (s^{-1})	K_{O2} (M^{-1})	ref
$[Cu(tmpa)(thf)]^+$	1.3×10^9	1.5×10^8	15.4	This work
$[Cu(tmpa)(EtCN)]^+$	5.8×10^7	1.5×10^7	0.38	11
$[Cu(Me\text{-}tmpa)]^+$	5×10^7	2.1×10^7	2.4	11
$[Cu(t\text{Bu-}tmpa)]^+$	1.6×10^8	9×10^7	1.7	11
$[Cu(MeO\text{-}tmpa)]^+$	7×10^7	1.3×10^7	5.5	11
$[Cu(tmpae)]^+$	4×10^7	4×10^8	0.10	48
$[Cu_2(D^1)]^+$	4×10^6	1.4×10^7	0.27	48
$[^2LCu]^+$	$>10^6$	N. A.	790	39
$[Cu(L^iPr3)]^{+a}$	1080	N. A.	N. A.	42
$[Cu(m\text{-}XYL^iPr4)]^{+a}$	20 800	N. A.	N. A.	42
$[Cu(i\text{-}Pr_4dtne)]^{+a}$	16 400	N. A.	N. A.	42
Hc monomer a[b]	4.6×10^7	410	1.12×10^5	45
Hc hexamer a[b]	3.1×10^7	190	1.63×10^5	45
Cu_B (C*c*O)	3.7×10^8	5×10^4	7×10^3	47
Tyrosinase[b]	2.3×10^7	1070	2.23×10^4	46
Range	10^6-10^9	10^2-10^8	$10^{-1}-10^5$	

[a] These form $\mu,\eta^2:\eta^2$/bis-μ-oxo dicopper(II) equilibrium mixtures. [b] These form $\mu,\eta^2:\eta^2$ peroxodicopper(II) products.

reaction and thus increasing the activation barrier. Consequently, the forward reaction "suffers" and the overall binding of dioxygen is not favored at room temperature as seen by the positive change in Gibbs free energy. As stated earlier, the solvent has no effect on the dissociation of dioxygen from the copper complex. All in all, the reaction in THF stabilizes the superoxide adduct by 40 times at room temperature and greater than 10^3 times at low temperatures.

A recent stopped-flow kinetic study by Schindler and Zuberbuhler[38] indicated that a related superoxo species, $[Cu^{II}(Me_6tren)(O_2^-)]^+$, is more stabilized than $[Cu^{II}(tmpa)(O_2^-)]^+$ in EtCN solvent (Table 1). The additional stability was attributed to the Me_6tren copper(I) compound's weaker nitrile adduct. This inefficient binding of a nitrile solvent resulted in a smaller activation enthalpy (17.1 kJ mol^{-1}, Table 1), yet this was compensated for by a significantly smaller activation entropy (-52 J mol^{-1} K^{-1}). Thus, a trend exists that is consistent with our data for $[Cu^{II}(tmpa)(O_2^-)]^+$ formation in THF. The activation enthalpy and entropy decrease as the solvent's influence on the copper system decreases. However, the rate constant for O_2 binding to $[Cu^I(Me_6tren)(EtCN)]^+$ in EtCN ($k_{O2} = 1.2 \times 10^7$ M^{-1} s^{-1}, extrapolated to 298 K) is smaller than the value we report here and is slightly smaller than our previous data in EtCN (refer to Table 1).[11]

There are relatively few other measurements for kinetics and thermodynamics of primary copper dioxygen adducts (Table 2). Tolman and Zuberbuhler recently reported the kinetics for the O_2-reaction of $[^2LCu^I]$ (Table 2) employing a tetradentate phenol ligand where they identified and characterized an unusually stabilized superoxo species (K_{O2}, 298 K = 790 M^{-1}).[39] The O_2-adduct was observed to form within the mixing time of the stopped-flow apparatus and thus, kinetic parameters could not be extracted. Studies of tridentate copper(I) complexes (i.e., $[Cu(L^{iPr3})]^+$, $[Cu_2(m\text{-}XYL^{iPr4})]^{2+}$, and $[Cu_2(i\text{-}Pr4dtne)]^{2+}$) forming the $\mu,\eta^2:\eta^2$-peroxo/bis-μ-oxo (2:1 Cu:O_2) complex mixtures exhibit rate limiting formation of an unobservable 1:1 Cu:O_2 species; a second copper(I) ion complex rapidly consumes this preformed intermediate.[40-42] Thus, values for k_{O2} have only been elucidated by steady-state models without any spectroscopic detection of superoxo species, and are orders of magnitude smaller (Table 2) than values reported here for cupric-superoxo species formation. Elucidation of binding constants was not possible due to the rate-limiting nature of the reaction.

Comparison of Copper and Heme Dioxygen Adducts. As mentioned, the methods described here to quantify Cu/O_2 interactions have been previously used by heme researchers. For natural and synthetic hemes, the rate constants for CO binding are smaller than for O_2, typically by 1 order of magnitude, e.g., 10^7 vs 10^8 M^{-1} s^{-1}.[8,24,25,43] Thus, for kinetic analyses of heme/O_2 interactions using eq 1, k_{CO}[CO] is deemed negligible and a plot of k_{fast} vs [O_2] is typically used to determine k_{O2}. This is in strong contrast to the present copper complex chemistry that indicates the opposite behavior, that $k_{CO} > k_{O2}$ in reactions of these gases with $[Cu^I(tmpa)(thf)]^+$. Direct comparison of $k_{O2} = 1.3 \times 10^9$ M^{-1} s^{-1} (298 K) for binding of O_2 to $[Cu^I(tmpa)(thf)]^+$ can be made with values for heme proteins and synthetic analogues, Table 3. *The second-order rate constant of O_2-binding to the copper center in $[Cu^I(tmpa)(thf)]^+$ exceeds that observed for reduced hemes.*[8,44]

It is also of interest to compare the kinetics of O_2-binding to $[Cu^I(tmpa)(thf)]^+$ to Cu-protein literature values, i.e., hemocyanin (O_2-carrier),[45] tyrosinase (monooxygenase)[46] and Cu_B at the heme-Cu active site of cytochrome *c* oxidase,[47] $k_{O2} \cong 10^7-10^8$ M^{-1} s^{-1} at 298 K (Table 2). *The k_{O2} for O_2-binding to $[Cu^I(tmpa)(thf)]^+$ exceeds previously reported Cu-protein values.* Our data thus supports the notion that O_2 could react faster with Cu_B than $heme_{a3}$, favoring the literature supposition that Cu_B acts as a "way stop"[47] for dioxygen binding to the $heme_{a3}$ site in cytochrome *c* oxidase. The thermodynamics of Cu$-O_2$ adduct formation also seem compatible. Hemocyanin, with two closely situated Cu-ions, favorably binds dioxygen ($K_{O2} = 10^5$ M^{-1}), similar to hemes and typical of a dioxygen carrier. However, Cu_B in cytochrome *c* oxidase has a smaller binding constant (7×10^3 M^{-1})[47] as it would need to release dioxygen to transfer to the $heme_{a3}$ portion. Similar to this situation, $[Cu^I(tmpa)(thf)]^+$ and other copper coordination compounds have small binding constants (10^{-1} to 10^2 M^{-1},

(38) Weitzer, M.; Schindler, S.; Brehm, G.; Hormann, E.; Jung, B.; Kaderli, S.; Zuberbuehler, A. D. *Inorg. Chem.* **2003**, *42*, 1800−1806.
(39) Jazdzewski, B. A.; Reynolds Anne, M.; Holland Patrick, L.; Young, V. G., Jr.; Kaderli, S.; Zuberbühler, A.; Tolman William, B. *J. Biol. Inorg. Chem.* **2003**, *8*, 381−393.
(40) Halfen, J. A.; Mahapatra, S.; Wilkinson, E. C.; Kaderli, S.; Young, V. G., Jr.; Que, L., Jr.; Zuberbühler, A. D.; Tolman, W. B. *Science* **1996**, *271*, 1397−1400.
(41) Tolman, W. B. *Acc. Chem. Res.* **1997**, *30*, 227−237.
(42) Mahapatra, S.; Kaderli, S.; Llobet, A.; Neuhold, Y.-M.; Palanché, T.; Halfen, J. A.; Young, V. G., Jr.; Kaden, T. A.; Que, L., Jr.; Zuberbühler, A. D.; Tolman, W. B. *Inorg. Chem.* **1997**, *36*, 6343−6356.
(43) Traylor, T. G.; Mitchell, M. J.; Tsuchiya, S.; Campbell, D. H.; Stynes, D. V.; Koga, N. *J. Am. Chem. Soc.* **1981**, *103*, 5234−5236.
(44) Wilkens, R. G. In *Oxygen Complexes and Oxygen Activation by Transition Metals*; Martell, A. E., Sawyer, D. T., Eds.; Plenum: New York, 1988; pp 49−60.
(45) Andrew, C. R.; McKillop, K. P.; Sykes, A. G. *Biochim. Biophys. Acta* **1993**, *1162*, 105−114.
(46) Rodriguez-Lopez, J. N.; Fenoll, L. G.; Garcia-Ruiz, P. A.; Varon, R.; Tudela, J.; Thorneley, R. N. F.; Garcia-Canovas, F. *Biochemistry* **2000**, *39*, 10 497−10 506.
(47) Varotsis, C.; Zhang, Y.; Appelman, E. H.; Babcock, G. T. *Proc. Natl. Acad. Sci. U.S.A.* **1993**, *90*, 237−241.
(48) Lee, D.-H.; Wei, N.; Murthy, N. N.; Tyeklár, Z.; Karlin, K. D.; Kaderli, S.; Jung, B.; Zuberbühler, A. D. *J. Am. Chem. Soc.* **1995**, *117*, 12 498−12 513.
(49) Collman, J. P.; Brauman, J. I.; Collins, T. J.; Iverson, B. L.; Lang, G.; Pettman, R. B.; Sessler, J. L.; Walters, M. A. *J. Am. Chem. Soc.* **1983**, *105*, 3038−3052.
(50) Ghiladi, R. A.; Kretzer, R. M.; Guzei, I.; Rheingold, A. L.; Neuhold, Y.-M.; Hatwell, K. R.; Zuberbühler, A. D.; Karlin, K. D. *Inorg. Chem.* **2001**, *40*, 5754−5767.
(51) Lavalette, D.; Momenteau, M. *J. Chem. Soc., Perkin Trans.* **1982**, 385−388.

Table 3. Kinetic and Thermodynamic Parameters for O_2 Reactions with Selected Synthetic and Natural Hemes (298 K)

compd	k_{O2} (M^{-1} s^{-1})	k_{-O2} (s^{-1})	K_{O2} (M^{-1})	ref
picket fence and pocket hemes	$0.22-43 \times 10^7$	9−46 000	$0.23-24.4 \times 10^4$	49
durene capped hemes	$0.98-10 \times 10^7$	$0.1-1.0 \times 10^5$	$0.82-1.0 \times 10^3$	24
chelated protoheme	6.2×10^7	4200	1.48×10^4	43
chelated mesoheme	5.3×10^7	1700	3.12×10^4	43
$(F_8TPP)Fe(EtCN)$	1.6×10^8	6×10^6	2.67×10^1	50
$(TPP)Fe(NH(CH_2)_3Im)$	5.0×10^7	2.5×10^4	2.00×10^3	51
$(Deut)Fe([O(CH_2)_3Py]$	2.0×10^8	7×10^4	2.86×10^3	51
myoglobin	$1.4-25 \times 10^7$	12−23 000	$0.74-117 \times 10^4$	8
hemoglobin	$2.9-22 \times 10^7$	21−620	$2.87-47.6 \times 10^5$	8
overall range	10^5-10^8	$10^{-1}-10^5$	10^2-10^6	

Table 2). Therefore, Cu(I) complexes bind dioxygen much *faster* than hemes but do not bind it as *tightly*.

Conclusion

Changing from a strongly coordinating nitrile solvent to the noncompeting solvent tetrahydrofuran enhances k_{O2} by more than 3 orders of magnitude at 198 K and twenty-five times at 298 K. This quantitative measure has been made possible by discovery of the photolability of $[Cu^I(tmpa)(CO)]^+$ and application of the "flash-and-trap" technique to a copper coordination compound, the first of its kind. Moreover, the present study reveals that while the thermodynamics of CO vs O_2-binding favor the former for both hemes and copper complexes, (i) $k_{CO} > k_{O2}$ for $[Cu^I(tmpa)(thf)]^+$ but $k_{CO} < k_{O2}$ for hemes,[24,25] and (ii) k_{O2} for a copper complex, $[Cu^I(tmpa)(thf)]^+$, exceeds that for hemes (proteins and synthetic) and copper proteins. To obtain further fundamental insights, future investigations will be aimed at extending the methods used here to other copper and heme copper complexes.

Acknowledgment. We acknowledge support from the Petroleum Research Fund (G.J.M.), a National Science Foundation environmental research grant (CRAEMS, K.D.K., and G.J.M.), and the National Institute of Health (K.D.K.).

Supporting Information Available: Eyring plots for the formation and dissociation of $[Cu^{II}(tmpa)(O_2^-)]^+$, Van't Hoff plot for the binding of O_2 to $[Cu^I(tmpa)(thf)]^+$, and an extended table of O_2-binding data for hemes. This material is available and free of charge via the Internet at http://pubs.acs.org.

JA034911V